PHYSICAL REVIEW B **94**, 020302(R) (2016)

Control of two-phonon correlations and the mechanism of high-wavevector phonon generation by ultrafast light pulses

T. Henighan,[1,2,*] M. Trigo,[1,3] M. Chollet,[4] J. N. Clark,[1,5] S. Fahy,[6,7] J. M. Glownia,[4] M. P. Jiang,[1] M. Kozina,[1] H. Liu,[1] S. Song,[4] D. Zhu,[4] and D. A. Reis[1,3,8,†]

[1]*Stanford PULSE Institute, SLAC National Accelerator Laboratory, Menlo Park, California 94025, USA*
[2]*Department of Physics, Stanford University, Stanford, California 94305-4060, USA*
[3]*SIMES Institute, SLAC National Accelerator Laboratory, Menlo Park, California 94025, USA*
[4]*Linac Coherent Light Source, SLAC National Accelerator Laboratory, Menlo Park, California 94025, USA*
[5]*Center for Free-Electron Laser Science, Deutsches Elektronensynchrotron, 22607 Hamburg, Germany*
[6]*Tyndall National Institute, Cork, Ireland*
[7]*Department of Physics, University College Cork, Cork, Ireland*
[8]*Department of Photon Science and Department of Applied Physics, Stanford University, Stanford, California 94305-4090, USA*

(Received 8 October 2015; revised manuscript received 13 June 2016; published 20 July 2016)

Impulsive optical excitation can generate both coherent and squeezed phonons through first- and second-order Raman-like processes. The expectation value of the phonon displacement $\langle u_q \rangle$ oscillates at the phonon mode frequency for the coherent state but remains zero for a pure squeezed state. In contrast, both show oscillations in $\langle |u_q|^2 \rangle$ at twice the phonon mode frequency. Therefore it can be difficult to distinguish them in a second-order measurement of the displacements as is typical in x-ray diffuse scattering. Here we demonstrate a simple method to distinguish the generation mechanism by measurement of the diffuse scattering following double-impulsive excitation. We find in the case of Ge and GaAs that the generation of large wavevector phonons spanning the Brillouin zone is dominated by a second-order process.

DOI: 10.1103/PhysRevB.94.020302

Light scattering in solids provides information about low-lying excitations, such as phonons [1–3]. Optical light scattering couples to low net momentum excitations because the wavelength of the light is large compared to the interatomic distances. In the case of first-order Raman scattering in perfect crystals, conservation of energy and crystal momentum dictates that the inelastically scattered photons involve the absorption or emission of a single phonon with reduced wavevector $\mathbf{q} \approx 0$. In second-order Raman scattering, the light couples to a broad continuum of phonon pairs with near equal and opposite momenta such that the reduced wavevector of each pair is near zero, but the individual phonons have $\mathbf{q}$ spanning the Brillouin zone (BZ). In the absence of perfect crystalline order, optical excitation can also couple to a disorder-activated first-order continuum [4]. Thus, it can be difficult to separate first- and second-order scatterings by measurement of the Raman spectrum alone.

An optical pump pulse can also excite a first-order Raman-active phonon if the pulse duration is significantly shorter than the phonon period [5,6]. Ideally this generates a coherent state in which the expectation value of the phonon displacement $\langle u_{\mathbf{q},\lambda} \rangle$ oscillates at the natural frequency of the mode (λ denotes the phonon branch) [7]. As in the case of frequency domain Raman, first-order impulsive optical scattering not only can couple to modes near the zone center in perfect crystals, but also can couple to high-wavevector modes in the presence of disorder. In the more general case of second-order-Raman-like processes, the short pump ideally generates a continuum of squeezed phonon pairs for which $\langle u_{\mathbf{q},\lambda} u_{-\mathbf{q},\lambda} \rangle = \langle |u_{\mathbf{q},\lambda}|^2 \rangle$ oscillates at twice the phonon frequencies for each $\mathbf{q}$ [8].

Recently we have demonstrated an optical-pump/x-ray probe time-domain analog of inelastic x-ray scattering [9]. In these measurements a femtosecond optical pump excites a broad continuum of phonons in the sample that are probed by oscillations in the x-ray diffuse scattering as a function of momentum transfer $\mathbf{K}$ and pump-probe delay t. The scattered x-ray intensity $I(\mathbf{K},t)$ is proportional to the energy-integrated dynamical structure factor [10] and thus a weighted sum of the second-order equal-time correlation functions $\langle u_{\mathbf{q},\lambda}(t) u_{-\mathbf{q},\lambda}(t) \rangle$ over λ at a given $\mathbf{q} = \mathbf{K} - \mathbf{G}$ (where $\mathbf{G}$ is the closest reciprocal lattice vector) [11,12]. The diffuse scattering was seen to oscillate at twice the transverse acoustic phonon frequencies as a function of $\mathbf{q}$ throughout the BZ [13] as expected for a second-order measurement in the phonon displacements. In Trigo *et al.* [9], the oscillations were attributed to scattering from squeezed phonon pairs generated (by second-order scattering) from the optical pump. However, both squeezed and coherent states would generate oscillations in the second-order correlation functions at twice the mode frequency so that the observation of the first overtone alone in the x-ray scattering cannot distinguish the excitation mechanism.

Here we propose and demonstrate a method for distinguishing first- and second-order generation mechanisms in a second-order measurement in the phonon displacements using femtosecond x-ray diffuse scattering. Our technique relies on two temporally separated optical pump pulses where the second pulse suppresses or amplifies the coherences initiated by the first depending on the observed oscillation frequency and time delay between the pumps [14–16]. We find that the patterns of suppression and amplification of the temporal

*henighan@slac.stanford.edu
†dreis@slac.stanford.edu

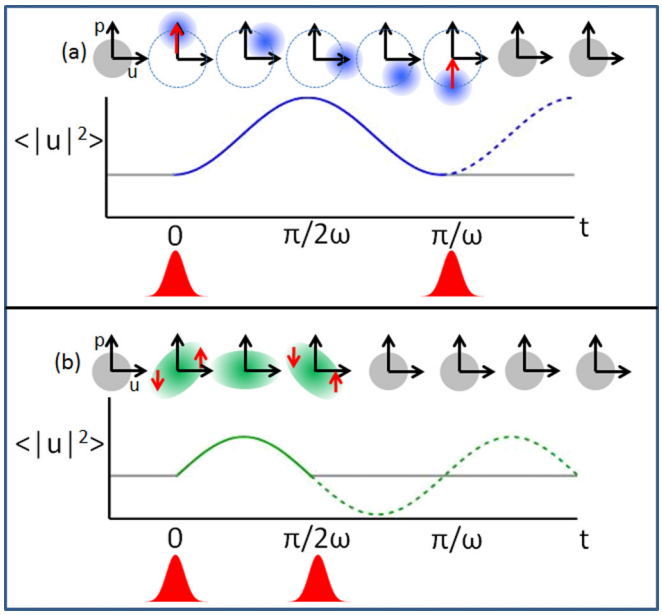

FIG. 1. Schematic of sudden excitation and deexcitation of coherent and squeezed modes, where ω is the phonon frequency. (a) Phase-space diagram of a phonon mode subjected to an impulse, generating a coherent state. An identical impulse at time π/ω later returns the mode to its original state. (b) Phonon mode of the same frequency subjected to a displacement-dependent impulse, generating a squeezed state. A second such displacement-dependent impulse at time $\pi/2\omega$ will return the mode to its original state. Note that in both cases, $\langle|u|^2\rangle$ oscillates at twice the phonon frequency. However, the delay between the two impulsive perturbations that will return the mode to its original state is different for the coherent and squeezed cases. The dashed and solid lines show the evolution of $\langle|u|^2\rangle$ in the absence and presence of the second pump pulse, respectively.

oscillations in the diffuse scattering following the second pump as a function of phonon frequency are consistent with the generation of high-wavevector squeezed phonons in the cases of undoped single-crystal Ge and GaAs. Our conclusion is based on the fact that the pump-pump delay required to suppress or amplify the temporal oscillations in $\langle|u_{\mathbf{q},\lambda}|^2\rangle$ differs for a squeezed and coherent state of the same mode as illustrated in Fig. 1 and discussed further below.

In quantum optics a coherent state is the right eigenstate of the annihilation operator which can be produced by applying the displacement operator on the ground state [17] and can be thought of as a classical state with added vacuum fluctuation noise [18] whereas a squeezed state often refers to a minimum uncertainty state in which the variance of one of the quadratures is less than the other but the product is given by the Heisenberg limit [18]. In general squeezing is not limited to a quantum phenomena [19], and classically arbitrary squeezing can be obtained for either quadrature [20]. Similarly, for our purposes we refer to a coherent state as one in which either the classical or quantum phase-space distribution is merely displaced from the origin, whereas a pure squeezed state is referred to as one in which the distribution is not displaced, but the variances are unequal [i.e., $\langle(\omega u)^2\rangle \neq \langle p^2\rangle$, where ω, u, and p are the phonon frequency, displacement, and momentum, respectively).

This Rapid Communication is concerned with the dynamical states of phonon modes. We treat these modes as independent classical harmonic oscillators that are perturbed by the pump pulses, although the results do not change significantly in a quantum treatment. Consider the simple case of a monatomic lattice in one dimension. We write phenomenologically the Hamiltonian for the single phonon branch interacting with optical radiation,

$$\begin{aligned} H &= \sum_q H_0(q) + \sum_q H_1(q,t) + \sum_{q,q'} H_2(q,q',t) \\ &= \sum_q \frac{1}{2}\left(p_q p_{-q} + \omega_q^2 u_q u_{-q}\right) + \sum_q A_1(q) f_1(t) u_q \\ &\quad + \sum_{q,q'} A_2(q,q') f_2(t) u_q u_{q'}. \end{aligned} \tag{1}$$

Here H_0 is the Hamiltonian for the unperturbed phonons in the harmonic approximation, and H_1 and H_2 represent the interaction of an optical field with single and pairs of phonons, respectively. u_q and p_q represent the normal mode coordinates and their conjugate momenta, respectively. In the case of nonresonant Raman processes $A_1(q)$ and $A_2(q,q')$ are proportional to the first- and second-order Raman susceptibilities, respectively, and $f_1(t) = f_2(t)$ is the pump pulse intensity.

By symmetry $A_1(q)$ is zero for a high wavevector in an ordered crystal, leaving H_2 as the leading-order interaction. Approximating the wavevector of the optical pump light as zero, momentum conservation imposes that A_2 is nonzero only when $q' = -q$. The disordered case, in contrast, can have finite A_1 even at high q [4]. To see how to distinguish these processes, consider how the pump pulses affect a single high-wavevector mode for which A_1 is nonzero. Utilizing the arguments above, noting that $u_{-q} = u_q^*$ and $p_{-q} = p_q^*$ [24], and treating u_q and p_q as classical variables, we obtain the equation of motion for a single oscillator,

$$\ddot{u}_q = -\omega^2 u_q - A_1(q) f_1(t) - 2A_2(q,-q) f_2(t) u_q. \tag{2}$$

For simplicity we assume the applied force is a δ function in time and that the oscillators are initially in a thermal distribution. We can think of this as a distribution of classical oscillators, and in this context $\langle|u|^2\rangle$ denotes the ensemble average of $|u|^2$ (i.e., the average over initial amplitudes and phases). Neglecting H_2 ($A_2 = 0$), the equation of motion contains an impulsive force from the A_1 term which displaces the phase-space distribution along the momentum (p) axis to generate a coherent state as illustrated in Fig. 1(a). In contrast, the impulsive force derived from the A_2 term is proportional to the oscillator displacement u. Thus if we neglect H_1 ($A_1 = 0$) the right $+u$ side of the distribution is pushed in the $+p$ direction, whereas the $-u$ side is pushed in the $-p$ direction, giving rise to a squeezed state as shown in Fig. 1(b). Although in this example we have considered only impulse-type excitation, displacive excitation is also possible, leading displacements along the u axes [25]. Thus the phase of the oscillations in $\langle|u|^2\rangle$ could take any value depending on the degree of impulsive and displacive excitations.

Figure 1 shows that $\langle|u|^2\rangle$ oscillates at *twice* the phonon frequency for *both* the squeezed and the coherent cases. Clearly a measurement of the frequency of oscillations in $I(\mathbf{K},t) \propto \langle|u_{\mathbf{q}=\mathbf{K}-\mathbf{G}}|^2\rangle$ following single pump excitation is not sufficient to distinguish these two dynamic states of the oscillator.

In Fig. 1 we also illustrate how coherent control of the phonon mode using two identical pump pulses could distinguish the aforementioned dynamical states in a second-order measurement of the phonon displacement. We start with a pair of equal-amplitude pulses separated by a fixed delay τ. We see that the coherent and squeezed motions are affected differently: To completely suppress the coherent phonon of natural frequency ω the second pulse has to arrive at delays $\tau = (2n+1)\pi/\omega$ for integer n (i.e., odd multiples of half the phonon period). On the other hand, to suppress the dynamics of the squeezed state of the same phonon mode the second pump has to arrive at $\tau = (2n+1)\pi/2\omega$ (i.e., odd multiples of $\frac{1}{4}$ of the *same* phonon period) in the limit of a sudden perturbative excitation [26]. Also note that suppressing one case leads to enhancing the other because of the $\frac{1}{4}$ cycle phase difference. This method yields a clear way to distinguish pure coherent versus pure squeezed states based on which frequencies are suppressed or enhanced for a given τ. For a general squeezed-coherent state, there is no τ which can completely suppress the oscillations.

Experiments were carried out at the x-ray pump-probe (XPP) instrument [27] of the Linac Coherent Light Source with a photon energy of 9.5 keV using a diamond double-crystal monochromater [28]. The x-ray pulses were less than 50 fs in duration and contained $\sim 10^9$ photons at a repetition rate of 120 Hz. Optical pulses of $\sim$65-fs duration were provided by a multipass Ti:sapphire amplifier centered at a wavelength of 800 nm. Delay between optical and x-ray pulses was controlled electronically and measured using the XPP timing tool, leading to an overall time resolution of $\sim$80 fs [29]. A Mach-Zehnder interferometer was used to control the delay between two collinear optical pump pulses of equal pulse energy. Scattering measurements were performed in a reflection geometry with x-ray grazing angles varying from 0.45° to 1.0° to match the optical and x-ray penetration depths for the various samples. The optical laser was 0.5° less grazing than the x rays and p polarized. The x-ray and optical laser beam cross sections were 200×15 and 600×90 μm^2, respectively. The samples were commercial single-crystal wafers of undoped Ge, GaAs, and InSb. Samples were mounted in a He-purged environment to minimize air scattering. Scattered x rays were collected using the Cornell-SLAC pixel array detector (CSPAD) on a shot-by-shot basis [30]. In each case, the sample orientation and detector position are fixed, and thus we probe a two-dimensional slice of reciprocal space. Each

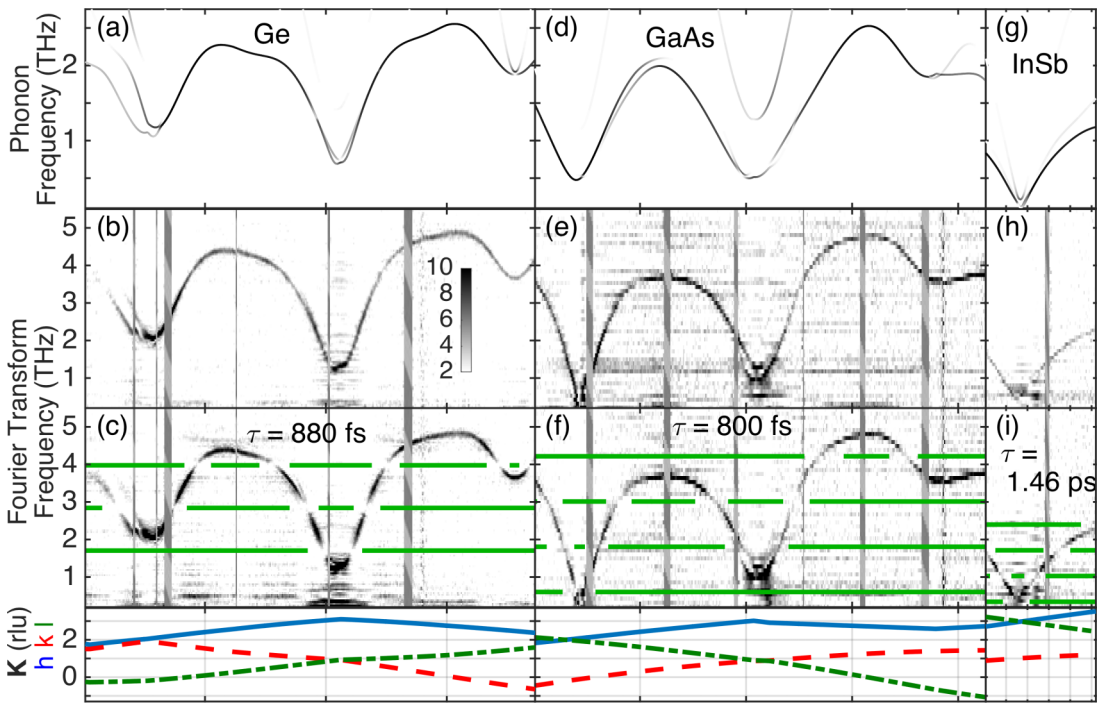

FIG. 2. Dispersion of $\langle|u_{\mathbf{q},\lambda}|^2\rangle$, matching twice the transverse-acoustic phonon branches, obtained by Fourier transform of temporal oscillations in the diffuse x-ray intensity following single and double optical pump excitations for (a)–(c) Ge, (d)–(f) GaAs, and (g)–(i) InSb. (b), (e), and (h) are with a single pump pulse, whereas (c), (f), and (i) are with two pumps where the pump-pump delay is labeled τ. The measured dispersions closely match twice the calculated acoustic phonon dispersions of (a), (d), and (g) using the force constants from Refs. [21–23] indicating our measurement is second order as expected. Line weights in (a), (d), and (g) indicate the squared structure factor and thus our expected sensitivity to the branch in the chosen geometry. The green horizontal lines in (c), (f), and (i) show frequencies which should be stopped by the second pulse for squeezed phonons. All measured dispersions have an identical color scale, shown in (b). The horizontal axis represents the scattering vector, the three components of which are shown in the top solid blue, dashed red, and dot-dashed green curves (in reciprocal lattice units). Vertical hashed bars are regions with no detector pixels. Note that the frequency never reaches zero because we did not probe the Γ point. This was by design to avoid Bragg peaks whose intensities would exceed the limits of the detector.

pixel on the CSPAD detector corresponds to a small spread in momentum transfer and thus crystal momentum set by the scattering geometry and the sample.

Figure 2 shows a portion of the measured dispersion of $\langle|u_{\mathbf{q},\lambda}|^2\rangle$ with single- and double-pump excitations in (a)–(c) Ge, (d)–(f) GaAs, and (g)–(i) InSb obtained using analysis described previously [9,13]. Here we have selected a one-dimensional path spanning multiple zones through the two-dimensional projection in reciprocal space. The dispersion is obtained by plotting the temporal Fourier transform of the differential change in $I(\mathbf{K},t)$ following the excitation by the pump pulse(s) for each pixel. The calculated dispersion along the same path is shown in Figs. 2(a), 2(d), and 2(f) where the weight of the lines represents the squared structure factor and thus our expected sensitivity to the branch in the chosen geometry. The observed dispersions match twice the frequency of the transverse-acoustic phonons in all three materials studied as expected for a measurement of $\langle|u_{\mathbf{q},\lambda}|^2\rangle$ and consistent with Refs. [9,13]. As seen in Fig. 2, the optical laser produces phonon coherences which span the BZ and have a continuum of frequencies. Thus if the phonon dispersion is known, a fixed pump-pump delay is in principle all that is necessary to distinguish squeezed from coherent motion assuming a single generation mechanism dominates. The second pulse excitation will maximally suppress the amplitude of the 2ω oscillations in $\langle|u_{\mathbf{q},\lambda}|^2\rangle$ only of those modes for which $\omega\tau \sim (2n+1)\pi/2$ if they are squeezed modes or $\omega\tau \sim (2n+1)\pi$ if they are coherent modes. The horizontal lines show twice the phonon frequencies which should be stopped by the second pulse if the phonons are squeezed. One clearly sees a decrease in the Fourier intensity at these frequencies when compared to the single pump for all three materials. This is consistent with the high-wavevector phonons being squeezed and thus generated by scattering of phonon pairs as represented by the interaction term H_2 in Eq. (1).

To more quantitatively test the generation mechanism, we compared the temporal Fourier-transform amplitude of the scattered signal after single- and double-pump excitations as a function of Fourier-transform frequency. Within the two-dimensional slice of reciprocal space probed, a mask was applied to exclude detector pixels with low scattering signals. Each unmasked pixel was assigned a frequency according to the maximum of its Fourier transform for the single-pump excitation, and data from pixels with the same frequency were combined. In Fig. 3, we plot the integrated Fourier peak for the double-pump excitation normalized to the single pump for each frequency bin. The error bars represent the standard mean error obtained when applying the same analysis to independent repeated measurements, whereas the points represent the average. Also shown is the calculated ratio for squeezed (green solid line) and coherent (blue dashed line) phonons assuming a δ-function excitation (in the case of a generalized coherent squeezed state, one would obtain a weighted superposition of these two curves). In Ge and GaAs, the data match the trends expected for squeezed phonons much more closely than those expected for coherent phonons. We conclude that the optical pump primarily generates pairs of phonons with nearly equal and opposite momenta in these two materials. However, the results from InSb are inconclusiv due to the relatively large statistical errors.

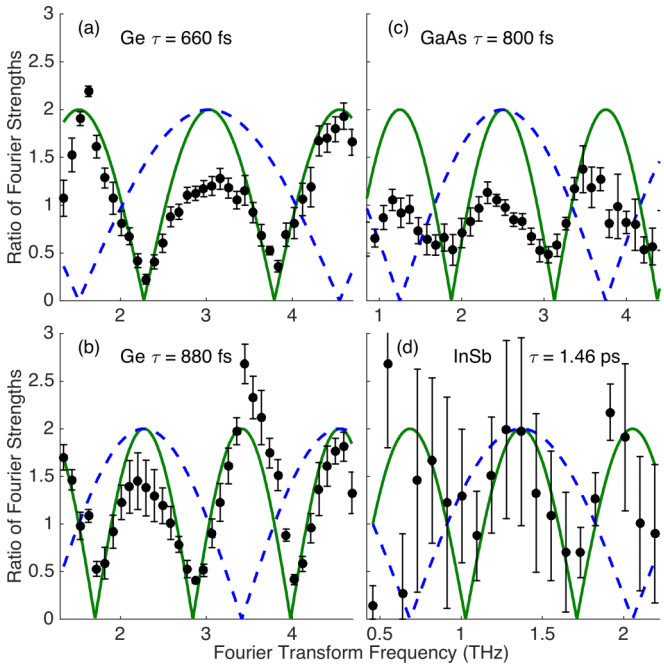

FIG. 3. Oscillation amplitude of phonon-phonon correlation (which oscillates at twice the phonon frequency, as seen in Fig. 2) following two-pulse excitation. The data is binned according to frequency and normalized to single-pulse excitation amplitude. The pump-pump delay is labeled τ. Solid green and dashed blue curves show expected trends for impulsive excitation for squeezed and coherent states, respectively, with no free parameters.

We emphasize that here we observe oscillations only at twice the phonon frequency. X-ray diffuse scattering can also detect $\langle\mathbf{u}_{\mathbf{q}}\rangle$ in first order in the presence of significant elastic scattering at $\mathbf{K} = \mathbf{G} + \mathbf{q}$. In this case the time-domain signal corresponds to a heterodyne detection between the elastic and the inelastically scattered x rays at a given momentum transfer and will thus oscillate at the phonon frequency for a coherent state [31]. In the case of disorder, we expect that the first-order continuum will be generated preferentially at the same momentum transfers that the elastic diffuse scattering is large. Therefore we expect a signal at both the fundamental and the second harmonic with their relative magnitudes depending on the details of the excitation and detection.

Our method for distinguishing first- and second-order phonon generations is valid for any time-resolved measurement of the second-order correlations in the atomic displacements. In the case of ultrafast optically excited Ge and GaAs, we confirm that the observed oscillations at twice the phonon frequency in the diffuse scattering signal are what is expected for squeezed as opposed to coherent phonon generation. This is consistent with the coherences in the second-order equal-time correlations $\langle|u_{\mathbf{q},\lambda}|^2\rangle$, being generated by a second-order process that creates correlated pairs of phonons with near equal and opposite momenta. This type of generation process is generally allowed by symmetry selection rules, making this method a broadly applicable technique for studying collective excitations in solids.

This work was primarily supported by the U.S. Department of Energy, Office of Science, Office of Basic Energy Sciences

through the Division of Materials Sciences and Engineering under Contract No. DE-AC02-76SF00515. Measurements were carried out at the Linac Coherent Light Source, a national user facility operated by Stanford University on behalf of the US Department of Energy, Office of Basic Energy Sciences. Preliminary measurements were performed at the BioCARS at the Advanced Photon Source. The Advanced Photon Source is supported by the U.S. Department of Energy, Basic Energy Sciences, Office of Science, under Contract No. DE-AC02-06CH11357. Use of BioCARS was also supported by the National Institutes of Health, National Institute of General Medical Sciences Grant No. 1R24GM111072. J.N.C. gratefully acknowledges financial support from the Volkswagen Foundation. S.F. acknowledges support by Science Foundation Ireland under Grant No. 12/IA/1601. D.A.R. acknowledges the SFI Walton Visitor award, Science Foundation Ireland Grant No. 11/1W/I2084, and discussions with R. Merlin. The authors also acknowledge P. Hillyard and E. Murray for their help with the calculated InSb dispersion.

[1] M. Cardona, *Light Scattering in Solids I* (Springer, Berlin, 1983).
[2] M. Cardona and G. Güntherodt, *Light Scattering in Solids IV* (Springer, Berlin, 1984).
[3] M. Cardona and R. Merlin, *Light Scattering in Solids IX* (Springer, Berlin, 2007).
[4] R. Carles, A. Zwick, M. Renucci, and J. Renucci, Solid State Commun. **41**, 557 (1982).
[5] L. Dhar, J. A. Rogers, and K. A. Nelson, Chem. Rev. **94**, 157 (1994).
[6] R. Merlin, Solid State Commun. **102**, 207 (1997).
[7] A. V. Kuznetsov and C. J. Stanton, Phys. Rev. Lett. **73**, 3243 (1994).
[8] G. Garrett, A. Rojo, A. Sood, J. Whitaker, and R. Merlin, Science **275**, 1638 (1997).
[9] M. Trigo, M. Fuchs, J. Chen, M. P. Jiang, M. Cammarata, S. Fahy, D. M. Fritz, K. Gaffney, S. Ghimire, A. Higginbotham, S. L. Johnson, M. E. Kozina, J. Larsson, H. Lemke, A. M. Lindenberg, G. Ndabashimiye, F. Quirin, K. Sokolowski-Tinten, C. Uher, G. Wang, J. S. Wark, D. Zhu, and D. A. Reis, Nat. Phys. **9**, 790 (2013).
[10] S. K. Sinha, J. Phys.: Condens. Matter **13**, 7511 (2001).
[11] In a thermal or number state, $\langle|u_{\mathbf{q},\lambda}|^2\rangle$ is equivalent to the mean-square displacement $\langle|u_{\mathbf{q},\lambda} - \langle u_{\mathbf{q},\lambda}\rangle|^2\rangle$.
[12] More generally, the energy-integrated dynamical structure factor is a weighted sum over $\langle u_{\mathbf{q},\lambda}(t)u_{-\mathbf{q},\lambda'}(t)\rangle$. The terms for which $\lambda \neq \lambda'$ can give rise to oscillations at the sum and difference frequencies of the two modes. Although such combination modes have not been observed in the tetrahedrally bonded semiconductors studied here, they were recently observed in photoexcited PbTe [32].
[13] D. Zhu, A. Robert, T. Henighan, H. T. Lemke, M. Chollet, J. M. Glownia, D. A. Reis, and M. Trigo, Phys. Rev. B **92**, 054303 (2015).
[14] M. Hase, K. Mizoguchi, H. Harima, S. Nakashima, M. Tani, K. Sakai, and M. Hangyo, Appl. Phys. Lett. **69**, 2474 (1996).
[15] M. F. DeCamp, D. A. Reis, P. H. Bucksbaum, and R. Merlin, Phys. Rev. B **64**, 092301 (2001).
[16] O. V Misochko, arXiv:1304.7485.
[17] R. J. Glauber, Phys. Rev. Lett. **10**, 84 (1963).
[18] R. Loudon and P. L. Knight, J. Mod. Opt. **34**, 709 (1987).
[19] V. Natarajan, F. DiFilippo, and D. E. Pritchard, Phys. Rev. Lett. **74**, 2855 (1995).
[20] D. Walls *et al.*, Nature (London) **306**, 141 (1983).
[21] F. Herman, J. Phys. Chem. Solids **8**, 405 (1959).
[22] T. Soma, H. Kagaya *et al.*, Phys. Status Solidi B **118**, 245 (1983).
[23] P. B. Hillyard, D. A. Reis, and K. J. Gaffney, Phys. Rev. B **77**, 195213 (2008).
[24] J. M. Ziman, *Principles of the Theory of Solids* (Cambridge University Press, Cambridge, UK, 1972).
[25] H. J. Zeiger, J. Vidal, T. K. Cheng, E. P. Ippen, G. Dresselhaus, and M. S. Dresselhaus, Phys. Rev. B **45**, 768 (1992).
[26] If the squeezing factor is large, the initial phase of the squeezed states deviates from the perturbative case. This in turn affects the pump-pump delay which achieves full suppression of the oscillations in $\langle|u|^2\rangle$.
[27] M. Chollet, R. Alonso-Mori, M. Cammarata, D. Damiani, J. Defever, J. T. Delor, Y. Feng, J. M. Glownia, J. B. Langton, S. Nelson *et al.*, J. Synchrotron Radiat. **22**, 503 (2015).
[28] D. Zhu, Y. Feng, S. Stoupin, S. A. Terentyev, H. T. Lemke, D. M. Fritz, M. Chollet, J. Glownia, R. Alonso-Mori, M. Sikorski *et al.*, Rev. Sci. Instrum. **85**, 063106 (2014).
[29] M. Harmand, R. Coffee, M. Bionta, M. Chollet, D. French, D. Zhu, D. Fritz, H. Lemke, N. Medvedev, B. Ziaja *et al.*, Nat. Photonics **7**, 215 (2013).
[30] P. Hart, S. Boutet, G. Carini, M. Dubrovin, B. Duda, D. Fritz, G. Haller, R. Herbst, S. Herrmann, C. Kenney *et al.*, *SPIE Optical Engineering+ Applications* (SPIE, Bellingham, WA, 2012), pp. 85040C.
[31] D. A. Reis and A. M. Lindenberg, in *Light Scattering in Solids IX, Topics in Applied Physics*, edited by M. Cardona and R. Merlin (Springer, Berlin, 2007), Vol. 108, pp. 371.
[32] M. P. Jiang *et al.*, Nature Commun., doi:10.1038/NCOMMS12291.